Search for Resonant WW and WZ Production in $p\bar{p}$ Collisions at $\sqrt{s} = 1.96$ TeV

V. M. Abazov,[35] B. Abbott,[72] B. S. Acharya,[29] M. Adams,[48] T. Adams,[46] G. D. Alexeev,[35] G. Alkhazov,[39] A. Alton,[60,*] G. Alverson,[59] G. A. Alves,[2] L. S. Ancu,[34] M. Aoki,[47] Y. Arnoud,[14] M. Arov,[57] A. Askew,[46] B. Åsman,[40] O. Atramentov,[64] C. Avila,[8] J. BackusMayes,[79] F. Badaud,[13] L. Bagby,[47] B. Baldin,[47] D. V. Bandurin,[46] S. Banerjee,[29] E. Barberis,[59] P. Baringer,[55] J. Barreto,[2] J. F. Bartlett,[47] U. Bassler,[18] V. Bazterra,[48] S. Beale,[6] A. Bean,[55] M. Begalli,[3] M. Begel,[70] C. Belanger-Champagne,[40] L. Bellantoni,[47] S. B. Beri,[27] G. Bernardi,[17] R. Bernhard,[22] I. Bertram,[41] M. Besançon,[18] R. Beuselinck,[42] V. A. Bezzubov,[38] P. C. Bhat,[47] V. Bhatnagar,[27] G. Blazey,[49] S. Blessing,[46] K. Bloom,[63] A. Boehnlein,[47] D. Boline,[69] T. A. Bolton,[56] E. E. Boos,[37] G. Borissov,[41] T. Bose,[58] A. Brandt,[75] O. Brandt,[23] R. Brock,[61] G. Brooijmans,[67] A. Bross,[47] D. Brown,[17] J. Brown,[17] X. B. Bu,[47] M. Buehler,[78] V. Buescher,[24] V. Bunichev,[37] S. Burdin,[41,†] T. H. Burnett,[79] C. P. Buszello,[40] B. Calpas,[15] E. Camacho-Pérez,[32] M. A. Carrasco-Lizarraga,[55] B. C. K. Casey,[47] H. Castilla-Valdez,[32] S. Caughron,[67] S. Chakrabarti,[69] D. Chakraborty,[49] K. M. Chan,[53] A. Chandra,[77] G. Chen,[55] S. Chevalier-Théry,[18] D. K. Cho,[74] S. W. Cho,[31] S. Choi,[31] B. Choudhary,[28] T. Christoudias,[42] S. Cihangir,[47] D. Claes,[63] J. Clutter,[55] M. Cooke,[47] W. E. Cooper,[47] M. Corcoran,[77] F. Couderc,[18] M.-C. Cousinou,[15] A. Croc,[18] D. Cutts,[74] M. Ćwiok,[30] A. Das,[44] G. Davies,[42] K. De,[75] S. J. de Jong,[34] E. De La Cruz-Burelo,[32] F. Déliot,[18] M. Demarteau,[47] R. Demina,[68] D. Denisov,[47] S. P. Denisov,[38] S. Desai,[47] K. DeVaughan,[63] H. T. Diehl,[47] M. Diesburg,[47] A. Dominguez,[63] T. Dorland,[79] A. Dubey,[28] L. V. Dudko,[37] D. Duggan,[64] A. Duperrin,[15] S. Dutt,[27] A. Dyshkant,[49] M. Eads,[63] D. Edmunds,[61] J. Ellison,[45] V. D. Elvira,[47] Y. Enari,[17] H. Evans,[51] A. Evdokimov,[70] V. N. Evdokimov,[38] G. Facini,[59] T. Ferbel,[68] F. Fiedler,[24] F. Filthaut,[34] W. Fisher,[61] H. E. Fisk,[47] M. Fortner,[49] H. Fox,[41] S. Fuess,[47] T. Gadfort,[70] A. Garcia-Bellido,[68] V. Gavrilov,[36] P. Gay,[13] W. Geist,[19] W. Geng,[15,61] D. Gerbaudo,[65] C. E. Gerber,[48] Y. Gershtein,[64] G. Ginther,[47,68] G. Golovanov,[35] A. Goussiou,[79] P. D. Grannis,[69] S. Greder,[19] H. Greenlee,[47] Z. D. Greenwood,[57] E. M. Gregores,[4] G. Grenier,[20] Ph. Gris,[13] J.-F. Grivaz,[16] A. Grohsjean,[18] S. Grünendahl,[47] M. W. Grünewald,[30] F. Guo,[69] G. Gutierrez,[47] P. Gutierrez,[72] A. Haas,[67,‡] S. Hagopian,[46] J. Haley,[59] L. Han,[7] K. Harder,[43] A. Harel,[68] J. M. Hauptman,[54] J. Hays,[42] T. Head,[43] T. Hebbeker,[21] D. Hedin,[49] H. Hegab,[73] A. P. Heinson,[45] U. Heintz,[74] C. Hensel,[23] I. Heredia-De La Cruz,[32] K. Herner,[60] G. Hesketh,[59] M. D. Hildreth,[53] R. Hirosky,[78] T. Hoang,[46] J. D. Hobbs,[69] B. Hoeneisen,[12] M. Hohlfeld,[24] S. Hossain,[72] Z. Hubacek,[10,18] N. Huske,[17] V. Hynek,[10] I. Iashvili,[66] R. Illingworth,[47] A. S. Ito,[47] S. Jabeen,[74] M. Jaffré,[16] S. Jain,[66] D. Jamin,[15] R. Jesik,[42] K. Johns,[44] M. Johnson,[47] D. Johnston,[63] A. Jonckheere,[47] P. Jonsson,[42] J. Joshi,[27] A. Juste,[47,§] K. Kaadze,[56] E. Kajfasz,[15] D. Karmanov,[37] P. A. Kasper,[47] I. Katsanos,[63] R. Kehoe,[76] S. Kermiche,[15] N. Khalatyan,[47] A. Khanov,[73] A. Kharchilava,[66] Y. N. Kharzheev,[35] D. Khatidze,[74] M. H. Kirby,[50] J. M. Kohli,[27] A. V. Kozelov,[38] J. Kraus,[61] A. Kumar,[66] A. Kupco,[11] T. Kurča,[20] V. A. Kuzmin,[37] J. Kvita,[9] S. Lammers,[51] G. Landsberg,[74] P. Lebrun,[20] H. S. Lee,[31] S. W. Lee,[54] W. M. Lee,[47] J. Lellouch,[17] L. Li,[45] Q. Z. Li,[47] S. M. Lietti,[5] J. K. Lim,[31] D. Lincoln,[47] J. Linnemann,[61] V. V. Lipaev,[38] R. Lipton,[47] Y. Liu,[7] Z. Liu,[6] A. Lobodenko,[39] M. Lokajicek,[11] P. Love,[41] H. J. Lubatti,[79] R. Luna-Garcia,[32,‖] A. L. Lyon,[47] A. K. A. Maciel,[2] D. Mackin,[77] R. Madar,[18] R. Magaña-Villalba,[32] S. Malik,[63] V. L. Malyshev,[35] Y. Maravin,[56] J. Martínez-Ortega,[32] R. McCarthy,[69] C. L. McGivern,[55] M. M. Meijer,[34] A. Melnitchouk,[62] D. Menezes,[49] P. G. Mercadante,[4] M. Merkin,[37] A. Meyer,[21] J. Meyer,[23] N. K. Mondal,[29] G. S. Muanza,[15] M. Mulhearn,[78] E. Nagy,[15] M. Naimuddin,[28] M. Narain,[74] R. Nayyar,[28] H. A. Neal,[60] J. P. Negret,[8] P. Neustroev,[39] S. F. Novaes,[5] T. Nunnemann,[25] G. Obrant,[39] J. Orduna,[32] N. Osman,[42] J. Osta,[53] G. J. Otero y Garzón,[1] M. Owen,[43] M. Padilla,[45] M. Pangilinan,[74] N. Parashar,[52] V. Parihar,[74] S. K. Park,[31] J. Parsons,[67] R. Partridge,[74,‡] N. Parua,[51] A. Patwa,[70] B. Penning,[47] M. Perfilov,[37] K. Peters,[43] Y. Peters,[43] G. Petrillo,[68] P. Pétroff,[16] R. Piegaia,[1] J. Piper,[61] M.-A. Pleier,[70] P. L. M. Podesta-Lerma,[32,¶] V. M. Podstavkov,[47] M.-E. Pol,[2] P. Polozov,[36] A. V. Popov,[38] M. Prewitt,[77] D. Price,[51] S. Protopopescu,[70] J. Qian,[60] A. Quadt,[23] B. Quinn,[62] M. S. Rangel,[2] K. Ranjan,[28] P. N. Ratoff,[41] I. Razumov,[38] P. Renkel,[76] P. Rich,[43] M. Rijssenbeek,[69] I. Ripp-Baudot,[19] F. Rizatdinova,[73] M. Rominsky,[47] C. Royon,[18] P. Rubinov,[47] R. Ruchti,[53] G. Safronov,[36] G. Sajot,[14] A. Sánchez-Hernández,[32] M. P. Sanders,[25] B. Sanghi,[47] A. S. Santos,[5] G. Savage,[47] L. Sawyer,[57] T. Scanlon,[42] R. D. Schamberger,[69] Y. Scheglov,[39] H. Schellman,[50] T. Schliephake,[26] S. Schlobohm,[79] C. Schwanenberger,[43] R. Schwienhorst,[61] J. Sekaric,[55] H. Severini,[72] E. Shabalina,[23] V. Shary,[18] A. A. Shchukin,[38] R. K. Shivpuri,[28] V. Simak,[10] V. Sirotenko,[47] P. Skubic,[72] P. Slattery,[68] D. Smirnov,[53] K. J. Smith,[66] G. R. Snow,[63] J. Snow,[71] S. Snyder,[70] S. Söldner-Rembold,[43] L. Sonnenschein,[21] A. Sopczak,[41] M. Sosebee,[75] K. Soustruznik,[9] B. Spurlock,[75] J. Stark,[14] V. Stolin,[36] D. A. Stoyanova,[38] M. Strauss,[72] D. Strom,[48] L. Stutte,[47] L. Suter,[43] P. Svoisky,[72] M. Takahashi,[43] A. Tanasijczuk,[1] W. Taylor,[6] M. Titov,[18] V. V. Tokmenin,[35] Y.-T. Tsai,[68] D. Tsybychev,[69] B. Tuchming,[18] C. Tully,[65] P. M. Tuts,[67] L. Uvarov,[39] S. Uvarov,[39] S. Uzunyan,[49] R. Van Kooten,[51] W. M. van Leeuwen,[33] N. Varelas,[48]

 © 2011 American Physical Society

E. W. Varnes,[44] I. A. Vasilyev,[38] P. Verdier,[20] L. S. Vertogradov,[35] M. Verzocchi,[47] M. Vesterinen,[43] D. Vilanova,[18] P. Vint,[42] P. Vokac,[10] H. D. Wahl,[46] M. H. L. S. Wang,[68] J. Warchol,[53] G. Watts,[79] M. Wayne,[53] M. Weber,[47,**] L. Welty-Rieger,[50] A. White,[75] D. Wicke,[26] M. R. J. Williams,[41] G. W. Wilson,[55] S. J. Wimpenny,[45] M. Wobisch,[57] D. R. Wood,[59] T. R. Wyatt,[43] Y. Xie,[47] C. Xu,[60] S. Yacoob,[50] R. Yamada,[47] W.-C. Yang,[43] T. Yasuda,[47] Y. A. Yatsunenko,[35] Z. Ye,[47] H. Yin,[47] K. Yip,[70] S. W. Youn,[47] J. Yu,[75] S. Zelitch,[78] T. Zhao,[79] B. Zhou,[60] J. Zhu,[60] M. Zielinski,[68] D. Zieminska,[51] and L. Zivkovic[67]

(D0 Collaboration)

[1]*Universidad de Buenos Aires, Buenos Aires, Argentina*
[2]*LAFEX, Centro Brasileiro de Pesquisas Físicas, Rio de Janeiro, Brazil*
[3]*Universidade do Estado do Rio de Janeiro, Rio de Janeiro, Brazil*
[4]*Universidade Federal do ABC, Santo André, Brazil*
[5]*Instituto de Física Teórica, Universidade Estadual Paulista, São Paulo, Brazil*
[6]*Simon Fraser University, Vancouver, British Columbia, and York University, Toronto, Ontario, Canada*
[7]*University of Science and Technology of China, Hefei, People's Republic of China*
[8]*Universidad de los Andes, Bogotá, Colombia*
[9]*Charles University, Faculty of Mathematics and Physics, Center for Particle Physics, Prague, Czech Republic*
[10]*Czech Technical University in Prague, Prague, Czech Republic*
[11]*Center for Particle Physics, Institute of Physics, Academy of Sciences of the Czech Republic, Prague, Czech Republic*
[12]*Universidad San Francisco de Quito, Quito, Ecuador*
[13]*LPC, Université Blaise Pascal, CNRS/IN2P3, Clermont, France*
[14]*LPSC, Université Joseph Fourier Grenoble 1, CNRS/IN2P3, Institut National Polytechnique de Grenoble, Grenoble, France*
[15]*CPPM, Aix-Marseille Université, CNRS/IN2P3, Marseille, France*
[16]*LAL, Université Paris-Sud, CNRS/IN2P3, Orsay, France*
[17]*LPNHE, Universités Paris VI and VII, CNRS/IN2P3, Paris, France*
[18]*CEA, Irfu, SPP, Saclay, France*
[19]*IPHC, Université de Strasbourg, CNRS/IN2P3, Strasbourg, France*
[20]*IPNL, Université Lyon 1, CNRS/IN2P3, Villeurbanne, France, and Université de Lyon, Lyon, France*
[21]*III. Physikalisches Institut A, RWTH Aachen University, Aachen, Germany*
[22]*Physikalisches Institut, Universität Freiburg, Freiburg, Germany*
[23]*II. Physikalisches Institut, Georg-August-Universität Göttingen, Göttingen, Germany*
[24]*Institut für Physik, Universität Mainz, Mainz, Germany*
[25]*Ludwig-Maximilians-Universität München, München, Germany*
[26]*Fachbereich Physik, Bergische Universität Wuppertal, Wuppertal, Germany*
[27]*Panjab University, Chandigarh, India*
[28]*Delhi University, Delhi, India*
[29]*Tata Institute of Fundamental Research, Mumbai, India*
[30]*University College Dublin, Dublin, Ireland*
[31]*Korea Detector Laboratory, Korea University, Seoul, Korea*
[32]*CINVESTAV, Mexico City, Mexico*
[33]*FOM-Institute NIKHEF and University of Amsterdam/NIKHEF, Amsterdam, The Netherlands*
[34]*Radboud University Nijmegen/NIKHEF, Nijmegen, The Netherlands*
[35]*Joint Institute for Nuclear Research, Dubna, Russia*
[36]*Institute for Theoretical and Experimental Physics, Moscow, Russia*
[37]*Moscow State University, Moscow, Russia*
[38]*Institute for High Energy Physics, Protvino, Russia*
[39]*Petersburg Nuclear Physics Institute, St. Petersburg, Russia*
[40]*Stockholm University, Stockholm and Uppsala University, Uppsala, Sweden*
[41]*Lancaster University, Lancaster LA1 4YB, United Kingdom*
[42]*Imperial College London, London SW7 2AZ, United Kingdom*
[43]*The University of Manchester, Manchester M13 9PL, United Kingdom*
[44]*University of Arizona, Tucson, Arizona 85721, USA*
[45]*University of California Riverside, Riverside, California 92521, USA*
[46]*Florida State University, Tallahassee, Florida 32306, USA*
[47]*Fermi National Accelerator Laboratory, Batavia, Illinois 60510, USA*
[48]*University of Illinois at Chicago, Chicago, Illinois 60607, USA*
[49]*Northern Illinois University, DeKalb, Illinois 60115, USA*
[50]*Northwestern University, Evanston, Illinois 60208, USA*

[51]Indiana University, Bloomington, Indiana 47405, USA
[52]Purdue University Calumet, Hammond, Indiana 46323, USA
[53]University of Notre Dame, Notre Dame, Indiana 46556, USA
[54]Iowa State University, Ames, Iowa 50011, USA
[55]University of Kansas, Lawrence, Kansas 66045, USA
[56]Kansas State University, Manhattan, Kansas 66506, USA
[57]Louisiana Tech University, Ruston, Louisiana 71272, USA
[58]Boston University, Boston, Massachusetts 02215, USA
[59]Northeastern University, Boston, Massachusetts 02115, USA
[60]University of Michigan, Ann Arbor, Michigan 48109, USA
[61]Michigan State University, East Lansing, Michigan 48824, USA
[62]University of Mississippi, University, Mississippi 38677, USA
[63]University of Nebraska, Lincoln, Nebraska 68588, USA
[64]Rutgers University, Piscataway, New Jersey 08855, USA
[65]Princeton University, Princeton, New Jersey 08544, USA
[66]State University of New York, Buffalo, New York 14260, USA
[67]Columbia University, New York, New York 10027, USA
[68]University of Rochester, Rochester, New York 14627, USA
[69]State University of New York, Stony Brook, New York 11794, USA
[70]Brookhaven National Laboratory, Upton, New York 11973, USA
[71]Langston University, Langston, Oklahoma 73050, USA
[72]University of Oklahoma, Norman, Oklahoma 73019, USA
[73]Oklahoma State University, Stillwater, Oklahoma 74078, USA
[74]Brown University, Providence, Rhode Island 02912, USA
[75]University of Texas, Arlington, Texas 76019, USA
[76]Southern Methodist University, Dallas, Texas 75275, USA
[77]Rice University, Houston, Texas 77005, USA
[78]University of Virginia, Charlottesville, Virginia 22901, USA
[79]University of Washington, Seattle, Washington 98195, USA

(Received 6 December 2010; revised manuscript received 3 March 2011; published 29 June 2011)

We search for resonant WW or WZ production by using up to 5.4 fb^{-1} of integrated luminosity collected by the D0 experiment in run II of the Fermilab Tevatron Collider. The data are consistent with the standard model background expectation, and we set limits on a resonance mass by using the sequential standard model W' boson and the Randall-Sundrum model graviton G as benchmarks. We exclude a sequential standard model W' boson in the mass range 180–690 GeV and a Randall-Sundrum graviton in the range 300–754 GeV at 95% C.L.

DOI: 10.1103/PhysRevLett.107.011801 PACS numbers: 12.60.Cn, 13.85.Rm, 14.70.Kv

The standard model of particle physics is expected to be a low energy effective theory valid for particle interactions below the TeV scale. Above this scale, extensions to the standard model (SM) augment the existing particle content, leading to enhanced production of many final states at colliders. Specifically, the production and decay of massive charged or neutral particles can produce an excess of W boson pairs for neutral particles or W and Z boson pairs for charged particles.

In this Letter, we search for resonant WW and WZ production by using data collected by the D0 detector from 1.96 TeV $p\bar{p}$ collisions produced by the Fermilab Tevatron Collider. We consider final states involving leptons and one or two jets, using a novel technique to reconstruct $W/Z \to$ jets decays. We use a sequential standard model (SSM) [1,2] W' boson as the benchmark for a WZ resonance and a Randall-Sundrum (RS) [3–5] graviton (G) resonance for the WW final state.

There are two recent direct searches for WZ or WW resonances by the CDF and D0 Collaborations that exclude WZ resonances with mass below 516 and 520 GeV, respectively, and an RS graviton $G \to WW$ resonance with mass less than 607 GeV [6,7]. Indirect searches for new physics in the WW and WZ diboson systems through measurements of the triple gauge couplings also show no deviation from the SM predictions [8–10]. The D0 Collaboration also excludes $M(W') < 1.00$ TeV [11], when assuming the W' boson decays as in the SM, and $M(G) < 1.05$ TeV [12], when assuming G decays into $\gamma\gamma$ or ee. The search for these resonances in the diboson decay channel covers the possibility that their coupling to leptons may be lower than the value predicted by the SM.

We obtain a combined result based on three independent searches: two new searches for resonant WW/WZ production with at least one jet and exactly one or two leptons in the final state using 5.4 fb^{-1} of integrated luminosity and

one search previously done on 4.1 fb^{-1} of integrated luminosity with three leptons in the final state [6]. We use data collected by the D0 experiment. A detailed description of the D0 detector can be found in Ref. [13]; we give only a brief description here. The innermost region is the tracking detector, which consists of silicon microstrip and central fiber trackers, both of which are surrounded by a solenoidal magnet producing a 2 T magnetic field. Charged particle tracks are formed from signals in these detectors. Surrounding the tracking detector are electromagnetic and hadronic calorimeters, both of which use liquid argon as the active medium. The calorimeters are housed in three cryostats that define the central region as $|\eta| < 1.1$ [14] and two end cap regions as $1.5 < |\eta| < 4$. Electrons are reconstructed in the electromagnetic calorimeter as isolated energy clusters, matched to tracks, and with a shower shape that is consistent with that of an electron. Jets are also formed in the calorimeters as clusters of energy in a cone with radius $\mathcal{R} = 0.5$ [15]. Finally, surrounding the calorimeters are central and forward muon systems in three layers consisting of precision wire chambers and fast scintillators used for triggering. Coverage of the muon system extends to $|\eta| \approx 2$. Located between the first and second layers of the muon system is a 1.8 T toroidal magnet, which allows an independent muon momentum measurement. A muon candidate is reconstructed as the combination of tracks in the muon system and the inner tracking detector and is required to be isolated from other tracks or calorimeter energy deposits.

We employ a Monte Carlo (MC) simulation to model all background processes except backgrounds from events not involving the decay of a W or Z boson, such as multijet production. The SSM W' boson, RS graviton, and SM diboson processes are simulated by using the PYTHIA [16] event generator, which generates the tree-level matrix element process and simulates subsequent particle showering and hadronization effects. Backgrounds from $t\bar{t}$, W + jets with $W \to \ell\nu$, and Z + jets with $Z \to \ell\ell$ are modeled by using the ALPGEN [17] generator, and single top quark production is modeled with the COMPHEP [18] generator. All generators are interfaced with PYTHIA for showering and hadronization. The ALPGEN-generated samples make use of the Mangano [19] jet-parton matching scheme to improve the jet multiplicity modeling. All MC samples are passed through a GEANT-based [20] simulation of the D0 detector and overlaid with data events from randomly selected bunch crossings to simulate multiple $p\bar{p}$ interactions within a single event. The signal samples are generated in exclusive final states with diboson resonance masses between 180 and 1250 GeV in 10 GeV steps up to 200 GeV and then 50 GeV steps above 200 GeV, by using the CTEQ6L1 [21] parton distribution functions. No interference between the SM W boson and the SSM W' boson production is included in the simulation since the effect is negligible [22]. All MC samples are normalized such that the predicted yield is equal to the production cross section multiplied by the integrated luminosity of the data. The W + jets and Z + jets samples are scaled to the product of the cross section calculated by ALPGEN and the k factor defined as the ratio of the next-to-leading order and leading order cross sections, which is computed by MCFM [23]. The $t\bar{t}$ events are normalized to a next-to-next-to-leading order calculation [24] with $m_t = 172.5$ GeV. Finally, the diboson samples are normalized to the next-to-leading order cross section predicted by MCFM, and the signal W' boson samples are normalized to the next-to-next-to-leading order cross sections [25]. The RS graviton samples are normalized to the PYTHIA-level cross section multiplied by a k factor of 1.3 [26].

Events in this search are placed in three mutually exclusive categories, thus maximizing signal sensitivity to each WW and WZ decay channel. The first category contains events with a leptonic decay of the W boson and hadronic decay of the W or Z boson. Events must contain exactly one electron or muon with transverse momentum $p_T > 20$ GeV, either one or two jets with $p_T > 20$ GeV, and missing transverse energy $\not\!\!E_T > 20$ GeV [27]. These events were collected by using triggers that require the presence of a high p_T lepton. Events with charged leptonic decays of the Z boson and hadronic decays of the W boson comprise the second category. These events must contain exactly two electrons or muons and exactly one or two jets with the same p_T thresholds as the first category. We require $\not\!\!E_T < 50$ GeV to remove mismeasured events and a dilepton mass between 70 and 110 GeV to select Z boson events. Both single lepton and dilepton triggers were used to collect events in this category. Fully leptonic decays of the WZ system constitute the final selection category. In this category any combination of three leptons (eee, $\mu\mu\mu$, $e\mu\mu$, $ee\mu$) with $p_T > 20$ GeV for each lepton is accepted. Additionally, $\not\!\!E_T > 30$ GeV is required. Events in this channel were collected by using the same set of triggers as the dilepton channel. More details of the trilepton analysis have been presented in a previous Letter [6].

In the first two selection categories, the background after the initial event selection is dominated by W or Z boson + jets, followed by multijet, $t\bar{t}$, single top quark, and diboson production. The multijet background, in both single lepton and dilepton events, is modeled by using data that fail the final lepton quality selection criteria. In single lepton events, the relative fraction of multijet (*fake*-lepton) background and all other backgrounds (*real*-lepton) is determined by measuring the relative rates at which each background type satisfies two different lepton quality criteria. In dilepton events, the sum of the MC-based backgrounds and the multijet background is normalized to data in the dilepton mass region between 40 and 70 GeV. The signal acceptance, in both single lepton and dilepton events, is estimated from the MC calculations and

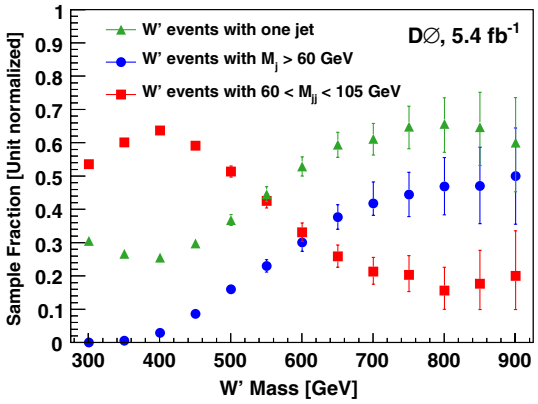

FIG. 1 (color online). The fraction of $W' \rightarrow WZ$ events with one reconstructed jet (triangles), events with a reconstructed jet mass (m_j) greater than 60 GeV (circles), and events with a dijet mass between 60 and 105 GeV (squares) as a function of the W' boson mass.

corrected for all data or MC differences and the estimated trigger selection efficiency.

The W and Z bosons result from the decay of a massive resonance and are therefore highly boosted. We exploit this property in the single lepton channel by requiring that the p_T of the lepton-E_T system be greater than 100 GeV and the azimuthal angle between the lepton and E_T be less than 1.5 rad. In the dilepton channel, we require that the dilepton pair p_T be greater than 100 GeV. The angular distance $\Delta\mathcal{R}$ between the two leptons must be less than 1.5, where the angular distance $\Delta\mathcal{R} = \sqrt{(\Delta\eta)^2 + (\Delta\phi)^2}$ is defined as the distance between the two objects in the pseudorapidity and azimuthal angle plane. The hadronically decaying W or Z boson in both single lepton and dilepton events will also be highly boosted. Given the extended size of jets, the two jets from the hadronic decay of W or Z bosons with sufficient transverse momentum may be merged in a single jet whose mass, defined in terms of the jet energy E_j and momentum $\vec{p}_j$ as $m_j = \sqrt{E_j^2 - |\vec{p}_j|^2}$, corresponds to the original boson mass. Thus, we further select events having a single jet with m_j greater than 60 (70) GeV when searching for a hadronically decaying W (Z) boson. If no jets satisfy these requirements, two isolated jets must be reconstructed in the event with a dijet mass between 60 and 105 GeV (70 and 115 GeV) for a W (Z) boson decay. In each channel, the $\Delta\mathcal{R}$ between the jets must be less than 1.5 rad. The relative fraction of signal events that satisfy the single jet and dijet mass requirements depends strongly on the assumed resonance mass. As seen in Fig. 1, events with a dijet mass between 60 and 105 GeV dominate the acceptance for low W' boson masses, and single massive jet events comprise most of the acceptance for high W' boson masses. Inclusion of the single jet with a large m_j final state results in an increase of the sensitivity for large W' masses in comparison to previous searches [7].

TABLE I. Expected event yields for the high-mass single lepton and dilepton selection samples. Uncertainties are combined statistical and systematic uncertainties on the background yields.

Process	Single lepton sample	Dilepton sample
Z + jets	3.6 ± 0.2	7.9 ± 0.8
W + jets	124.5 ± 20.3	<0.01
Top	22.9 ± 2.5	<0.01
Multijet	4.6 ± 0.3	<0.01
Diboson	27.6 ± 1.4	0.8 ± 0.1
Background sum	183.2 ± 24.5	8.7 ± 0.8
Data	174	8

We increase the search sensitivity by subdividing all search channels into "high"-mass and "low"-mass signal regions, where the mass refers to the assumed signal mass (M_{res}) and high-mass and low-mass are defined as $M_{\text{res}} \geq 450$ and <450 GeV, respectively. The low-mass signal region is composed of all events that satisfy the single lepton and dilepton selection requirements. In the high-mass signal region we additionally require the lepton-E_T system $p_T > 150$ GeV and the azimuthal angle difference between the lepton and E_T to be less than 1.0 rad for single lepton events. The dilepton high-mass selection requires the dilepton p_T to be greater than 150 GeV and the $\Delta\mathcal{R}$ between the two leptons must be less than 1.0 rad. Table I displays the estimated background yields, the expected numbers of signal events, and the numbers of observed data events after the high-mass selection. Figures 2 and 3 compare the data with the estimated backgrounds in the single lepton and dilepton channels using the reconstructed resonance mass and transverse mass [28], respectively.

The dominant systematic uncertainties on the background normalization and signal acceptance in the dilepton channel are mostly due to the Z + jets cross section (10%)

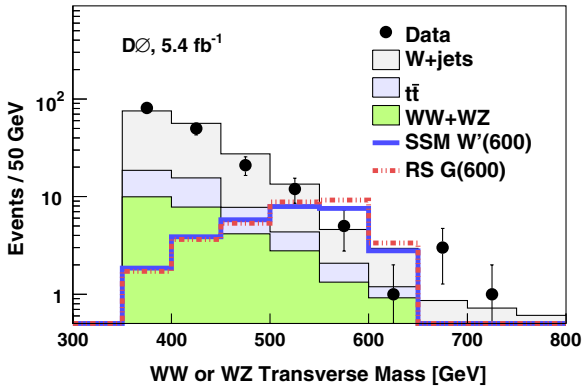

FIG. 2 (color online). The reconstructed WW or WZ transverse mass distribution for the data (points) with statistical error bars and the estimated backgrounds in the single lepton channel. The predicted SSM W' distribution for $M(W') = 600$ GeV and the RS graviton distribution for $M(G) = 600$ GeV are shown as solid and dashed lines, respectively.

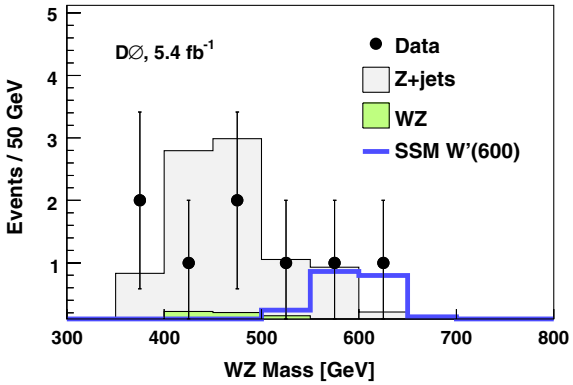

FIG. 3 (color online). The reconstructed WZ mass distribution for the data (points) with statistical error bars and the estimated backgrounds, and the predicted SSM W' distribution for $M(W') = 600$ GeV in the dilepton channel.

and to jet energy resolution (3%) effects. The main sources of systematic uncertainties in single lepton events are the W + jets (15%) and $t\bar{t}$ cross section (10%) and the integrated luminosity (6.1%) [29]. In single jet events in both single lepton and dilepton channels, the principal uncertainty is due to the m_j modeling in the Monte Carlo simulations. This uncertainty is 10% for jet masses below 30 GeV and rises to 25% for masses near 60 GeV. To determine it, a control region is defined from events satisfying the initial event selection but failing the lepton-E_T or the dilepton system $p_T > 100$ GeV requirement. The relative difference between the background prediction and the data is 10% for jet masses below 30 GeV and rises to 25% for masses near 60 GeV. We do not observe any event with jets having a mass greater than 60 GeV in the control region.

No statistically significant excess of the data over the background prediction is observed. Thus, we set limits on the production cross section multiplied by the branching ratio by using a modified frequentist approach [30]. In this method a log-likelihood ratio test statistic [31] is formed by using the Poisson probabilities for estimated background yields, the signal acceptance, and the observed number of events for all resonant mass hypotheses. Confidence levels are derived by integrating the log-likelihood ratio in pseudoexperiments using both the signal plus background hypotheses (CL_{s+b}) as well as the background only hypothesis (CL_b). In the modified frequentist approach, the excluded production cross section is computed as the cross section for which CL_s, defined as CL_{s+b}/CL_b, is equal to 0.05. Limits on the WZ resonance are set by using the distribution of the reconstructed mass in dilepton events and of the reconstructed transverse mass in single lepton events, with a bin size of 50 GeV. The W' signal acceptance and the expected background yield are parametrized accordingly. A similar procedure is used to set limits on the RS graviton signal by using the reconstructed transverse mass in single lepton events. We exclude an SSM W' boson in the mass region between 180 and 690 GeV and an RS graviton in the mass range of 300–754 GeV at 95% C.L. The graviton mass exclusion assumes the dimensionless coupling parameter $k/\bar{M}_{\rm pl} = 0.1$, where k is the curvature scale of the warped extra dimension and $\bar{M}_{\rm pl} = M_{\rm pl}/\sqrt{8\pi}$ is the reduced Planck mass. The expected and observed excluded cross sections for both the SSM W' boson and RS graviton as a function of the signal resonance mass are shown in Fig. 4.

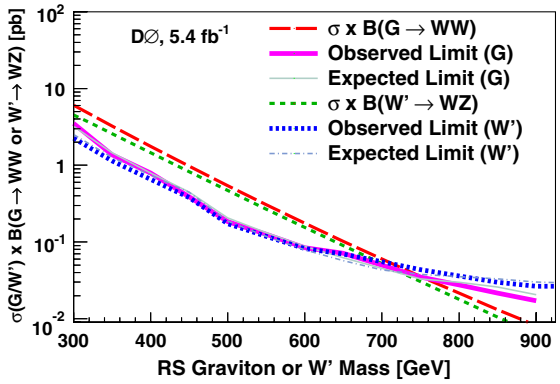

FIG. 4 (color online). The excluded production cross section for an SSM W' boson and the RS graviton as a function of the W' boson mass or graviton mass. The excluded mass region is the region where the SSM W' boson or RS graviton cross section exceeds the excluded cross section.

In this analysis we assume a linear relationship between the resonance mass and total width and that the width is smaller than the expected experimental mass resolution. In some classes of models, the total width grows as a power of the mass, yielding widths larger than the expected mass resolution. Using PYTHIA $W' \rightarrow WZ$ MC events with varying W' boson widths, we observe that our results are valid for widths below 10% of the resonance mass or, alternatively, for a coupling strength at the $W'WZ$ vertex up to 10 times the SSM value.

In summary, with up to 5.4 fb^{-1} of Tevatron run II integrated luminosity we do not observe an excess of events over the SM background prediction for events in WW and WZ boson final states. We set limits on the production cross section multiplied by the branching ratio for resonant WW and WZ boson pair production by using two theoretical benchmark scenarios: SSM $W' \rightarrow WZ$ and RS $G \rightarrow WW$ production. Under these assumptions, we exclude an SSM W' boson with a mass between 180 and 690 GeV and an RS graviton with a mass between 300 and 754 GeV at 95% C.L. Our novel use of the jet mass to select hadronic decays of the W and Z bosons was essential to obtaining such stringent limits, which are the best for these new physics scenarios.

We thank the staffs at Fermilab and collaborating institutions and acknowledge support from the DOE and NSF (USA); CEA and CNRS/IN2P3 (France); FASI, Rosatom,

and RFBR (Russia); CNPq, FAPERJ, FAPESP, and FUNDUNESP (Brazil); DAE and DST (India); Colciencias (Colombia); CONACyT (Mexico); KRF and KOSEF (Korea); CONICET and UBACyT (Argentina); FOM (The Netherlands); STFC and the Royal Society (United Kingdom); MSMT and GACR (Czech Republic); CRC Program and NSERC (Canada); BMBF and DFG (Germany); SFI (Ireland); The Swedish Research Council (Sweden); and CAS and CNSF (China).

*Visitor from Augustana College, Sioux Falls, SD, USA.
†Visitor from The University of Liverpool, Liverpool, United Kingdom.
‡Visitor from SLAC, Menlo Park, CA, USA.
§Visitor from ICREA/IFAE, Barcelona, Spain.
‖Visitor from Centro de Investigacion en Computacion—IPN, Mexico City, Mexico.
¶Visitor from ECFM, Universidad Autonoma de Sinaloa, Culiacán, Mexico.
**Visitor from Universität Bern, Bern, Switzerland.

[1] J. C. Pati and A. Salam, Phys. Rev. D **10**, 275 (1974); **11**, 703(E) (1975).
[2] G. Altarelli, B. Mele, and M. Ruiz-Altaba, Z. Phys. C **45**, 109 (1989); **47**, 676(E) (1990).
[3] L. Randall and R. Sundrum, Phys. Rev. Lett. **83**, 3370 (1999).
[4] L. Randall and R. Sundrum, Phys. Rev. Lett. **83**, 4690 (1999).
[5] H. Davoudiasl, J. L. Hewett, and T. G. Rizzo, Phys. Rev. D **63**, 075004 (2001).
[6] V. M. Abazov *et al.* (D0 Collaboration), Phys. Rev. Lett. **104**, 061801 (2010).
[7] T. Aaltonen *et al.* (CDF Collaboration), Phys. Rev. Lett. **104**, 241801 (2010).
[8] V. M. Abazov *et al.* (D0 Collaboration), Phys. Rev. Lett. **103**, 191801 (2009).
[9] V. M. Abazov *et al.* (D0 Collaboration), Phys. Rev. D **80**, 053012, (2009).
[10] The LEP Collaborations ALEPH, DELPHI, L3, and OPAL, http://lepewwg.web.cern.ch/LEPEWWG/lepww/tgc/summer03/gc_main2003.ps.
[11] V. M. Abazov *et al.* (D0 Collaboration), Phys. Rev. Lett. **100**, 031804 (2008).
[12] V. M. Abazov *et al.* (D0 Collaboration), Phys. Rev. Lett. **104**, 241802 (2010).
[13] V. M. Abazov *et al.* (D0 Collaboration), Nucl. Instrum. Methods Phys. Res., Sect. A **565**, 463 (2006); M. Abolins *et al.*, Nucl. Instrum. Methods Phys. Res., Sect. A **584**, 75 (2008); R. Angstadt *et al.*, Nucl. Instrum. Methods Phys. Res., Sect. A **622**, 298 (2010).
[14] The D0 detector utilizes a right-handed coordinate system with the z axis pointing in the direction of the proton beam and the y axis pointing upwards. The azimuthal angle ϕ is defined in the xy plane measured from the x axis. The pseudorapidity is defined as $\eta = -\ln[\tan(\theta/2)]$, where $\theta = \arctan(\sqrt{x^2 + y^2}/z)$. The transverse variables are defined as projections of the variables onto the xy plane.
[15] G. C. Blazey *et al.*, in *Proceedings of the Workshop: QCD and Weak Boson Physics in Run II*, edited by U. Baur, R. K. Ellis, and D. Zeppenfeld, Report No. Fermilab-Pub-00/297, 2000 (unpublished).
[16] T. Sjöstrand, S. Mrenna, and P. Skands, J. High Energy Phys. 05 (2006) 026; we used version 6.419 with TUNE A.
[17] M. L. Mangano *et al.*, J. High Energy Phys. 07 (2003) 001.
[18] E. Boos *et al.*, Nucl. Instrum. Methods Phys. Res., Sect. A **534**, 250 (2004).
[19] S. Hoche *et al.*, arXiv:0602.031.
[20] R. Brun and F. Carminati, CERN Program Library Long Writeup W5013, 1993.
[21] J. Pumplin *et al.*, J. High Energy Phys. 07 (2002) 012.
[22] T. G. Rizzo, J. High Energy Phys. 05 (2007) 037.
[23] J. Campbell and R. K. Ellis, Phys. Rev. D **65**, 113007 (2002); J. Campbell, R. K. Ellis, and D. Rainwater, Phys. Rev. D **68**, 094021 (2003).
[24] S. Moch and P. Uwer, Phys. Rev. D **78**, 034003 (2008).
[25] R. Hamburg, W. L. van Neerven, and T. Matsuura, Nucl. Phys. **B359**, 343 (1991); **B644**, 403(E) (2002).
[26] V. Ravindran and J. Smith, Phys. Rev. D **76**, 114004 (2007).
[27] The missing transverse energy, denoted as E_T in the text, is the imbalance of the momentum estimated from the calorimeter and reconstructed muons in the xy plane.
[28] The transverse mass of a particle with N decay products is defined as $M_T = \sqrt{\sum_i^N (E_T^i)^2 - (p_x^i)^2 - (p_y^i)^2}$.
[29] T. Andeen *et al.*, Report No. FERMILAB-TM-2365, 2007.
[30] W. Fisher *et al.* (D0 Collaboration), Report No. FERMILAB-TM-2386-E, 2006.
[31] T. Junk, Nucl. Instrum. Methods Phys. Res., Sect. A **434**, 435 (1999); A. Read, J. Phys. G **28**, 2693 (2002).